Estimation and Prediction of Drug Therapy on the Termination of Atrial Fibrillation by Autoregressive Model With Exogenous Inputs

Chin-En Kuo, Sheng-Fu Liang, *Member, IEEE*, Shao-Sheng Lu, Tang-Ching Kuan, and Chih-Sheng Lin

***Abstract*—Atrial fibrillation (AF) is the most frequent cardiac arrhythmia seen in clinical practice. Several therapeutical approaches have been developed to terminate the AF and the effects are evaluated by the reduction of the wavelet number after the treatments. Most of the previous studies focus on modeling and analysis of the mechanism, and the characteristic of AF. But no one discusses about the prediction of the result after the drug treatment. This paper is the first study to predict whether the drug treatment for AF is active or not. In this paper, the linear autoregressive model with exogenous inputs (ARX) that models the system output–input relationship by solving linear regression equations with least-squares method was developed and applied to estimate the effects of pharmacological therapy on AF. Recordings (224-site bipolar recordings) of plaque electrode arrays placed on the right and left atria of pigs with sustained AF induced by rapid atrial pacing were used to train and test the ARX models. The cardiac mapping data from 12 pigs treated with intravenous administration of antiarrhythmia drug, propafenone (PPF), or *dl*-sotalol (STL) were evaluated. The recordings of cardiac activity before the drug treatment were input to the model and the model output reported the estimated wavelet number of atria after the drug treatment. The results show that the predicting accuracy rate corresponding to the PPF and STL treatments was 100% and 92%, respectively. It is expected that the developed ARX model can be further extended to assist the clinical staffs to choose the effective treatments for the AF patients in the future.**

***Index Terms*—Atrial fibrillation (AF), autoregressive model with exogenous inputs (ARX), pharmacological therapy, wavelet number.**

I. Introduction

ATRIAL fibrillation (AF) is a serious arrhythmia associated with morbidity and mortality. The prevalence of AF is 0.4% of the general population. AF is more frequent in the elderly, as its prevalence doubles with each decade of age, from 0.5% at ages between 50 and 59 years to almost 9% at ages between 80 and 89 years [1], [2]. During AF, various regions of the atrial wall pulse to 400–600 beats per minute (bpm). If the atrial impulses were conducted to the ventricles, the extremely rapid ventricular rate would lead to ineffective cardiac contraction and rapid death. Several cardiac disorders predispose to AF, including coronary artery disease, pericarditis, mitral valve disease, congenital heart disease, congestive heart failure, thyrotoxic heart disease, and hypertension [3]. These considerations probably account for the significant role of AF in the occurrence of stroke: AF is the single most important cause of ischemic stroke in people older than 75 [4].

There are three general strategies for management of patients with AF, including 1) restoration and maintenance of sinus rhythm; 2) control of ventricular rate; and 3) prevention of stroke [5], [6]. Either pharmacologic or nonpharmacologic options can be chosen in certain situations. However, the restoration and maintenance of sinus rhythm is the best physiological strategy in the management of AF [7]. The maintenance of sinus rhythm can be divided into pharmacologic and nonpharmacologic options. In this paper, we discussed the effect of restoring sinus rhythm in the pigs with sustained AF by the treatment of pharmacologic approach, i.e., the AF pigs were treated with antiarrhythmia drug, propafenone (PPF), or *dl*-sotalol (STL). PPF can slow the conduction of nerve impulses in the heart and reduce the sensitivity of heart tissue to specific nerve impulses, which helps to stabilize heartbeat. PPF also has weak beta-blocking properties. STL is a beta-block drug. STL prolongs the atrial action potential duration by blocking the delayed rectifier potassium channel, but its effect declines at a rapid rate with reverse-use dependence [8]. STL significantly increases the effective refractory period [9]. The sotalol and propafenon chosen for this study are according to the ACC/AHA practice guidelines for the management of patients with AF, in which "in patients with lone AF, a beta-blocker may be tried first, but flecainide, propafenone, and sotalol are particularly effective." is indicated [10]. In our study, the pigs were treated by rapid atrial pacing and "lone" AF was induced.

Many methods have been proposed to understand the mechanism of AF and evaluate the terminating factors of AF [11]–[18]. However, most of the previous studies focus on modeling and analysis of the mechanism, and the characteristic of AF. But the discussion about the changes of the electrogram after the pharmacologic treatment is rare. The objective of this paper is

Manuscript received November 8, 2011; revised March 8, 2012 and May 30, 2012; accepted October 7, 2012. Date of current version February 4, 2013. This work was supported in part by the National Science Council of Taiwan under Grant NSC 98-2313-B-009-002-MY3, Grant NSC 100-2911-I-009-101, and Grant NSC 101-2220-E-006-010.

C.-E. Kuo and S.-S. Lu are with the Department of Computer Science and Information Engineering, National Cheng Kung University, Tainan 701, Taiwan (e-mail: chihen.kuo@gmail.com; p7696107@mail.ncku.edu.tw).

S.-F. Liang is with the Department of Computer Science and Information Engineering and the Institute of Medical Informatics, National Cheng Kung University, Tainan 701, Taiwan (e-mail: sfliang@mail.ncku.edu.tw).

T.-C. Kuan and C.-S. Lin are with the Department of Biological Science and Technology, National Chiao Tung University, Hsinchu 300, Taiwan (e-mail: yusi.kuan@gmail.com; lincs@mail.nctu.edu.tw).

Color versions of one or more of the figures in this paper are available online at http://ieeexplore.ieee.org.

Digital Object Identifier 10.1109/TITB.2012.2224877

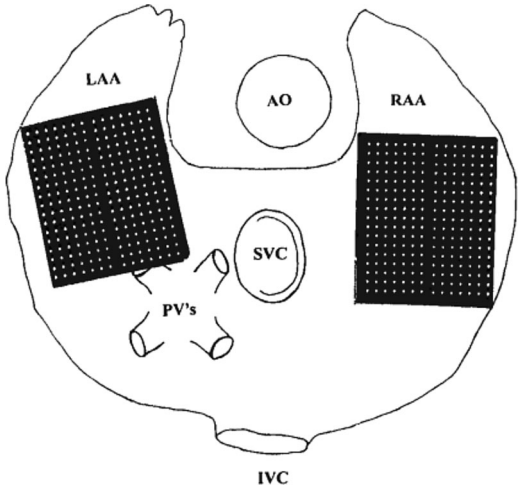

Fig. 1. Sketch showing the locations of plaque electrode mapping (14 × 16) in the LA and RA of the pig model. AO = aorta; IVC = inferior vena cava; LAA = LA appendage; PV's = convergence of pulmonary vein orifices; RAA = RA appendage; and SVC = superior vena cava [19].

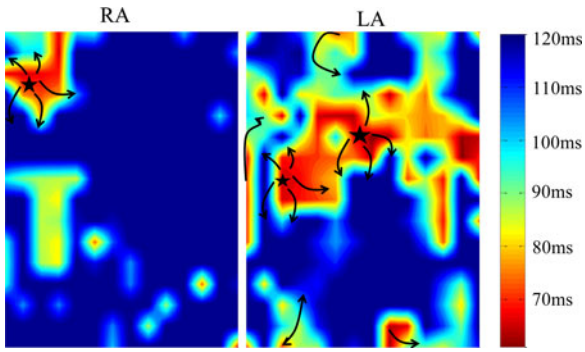

Fig. 2. Example of biatrial activation mapping with the plaque electrode. Isochronal maps are drawn to maximize temporal differences in color. Red represents the earliest of activation and deep blue represents the latest (see the vertical bars). The left figure represents the RA and right figure represents the LA. The asterisk means the epicardial breakthrough and the arrows represent the direction of wavelet propagation.

to estimate the conditions and characteristics of electrogram after the pharmacologic treatments in the pig AF model [19]. The nonlinear method was utilized to analyze the difference between before and after the drug treatment of PPF and STL. The ARX model was developed to predict the oscillation of the atrial activation (AA) interval series after the treatment by feeding the recordings before the treatment as the input. After that, the estimated wavelet number could be calculated to assess the effects after medication. Moreover, we could set two thresholds as -2.5 and -1.7 to predict whether the PPF and STL administrations are working or not by the results of our experiment, respectively.

II. Materials and Methods

A. Subjects and Data Acquisition

Twelve female pigs of Yorkshire–Landrace strain (average weight of 65 kg) were implanted with a high-speed atrial pacemaker (Itrel-III, model 7425; Medtronic Inc., Minneapolis, MN) for continuous pacing at 400–600 bpm for 4–6 weeks. Consistency of atrial pacing was regularly checked daily in the first week and twice weekly thereafter by a portable ECG monitor. After 4–6 weeks of continuous atrial pacing, sustained AF and free from significant heart failure were induced. Sustained AF was defined as persistent AF lasting at least 24 h after atrial pacing was terminated [19], [20]. Epicardial mapping of sustained AF was performed sequentially on the right atrium (RA) and the left atrium (LA) by a rectangular plaque electrode (62×52 mm^2; Prucka Engineering Inc., Houston, TX), which contains 224-site (14×16) bipolar recordings by paired connections (see Fig. 1). The epicardial mapping for RA and LA was separately detected; therefore, we treated the data by RA and LA independently. The data were sampled at 1 kHz. The intrabipolar and interbipolar distances were 3.5 mm. The epicardial mapping of each subject has repeatedly recorded and each event was recorded continuously for at least 30 s. The circuits were dynamically generated, but stably dominant frequency of activation and wavelet number could be found.

There were five pigs with the PPF treatment and seven pigs with the STL treatment. The activation time of each local electrogram on each recording channel was assigned automatically at the maximum dv/dt and subsequently edited manually. The sequence of the interval between two consecutive atrial stimuli (AA interval) was calculated from the differentiation of activation time sequence. The minimal local AA intervals in the local activation time were chosen to represent the minimal acceptable atrial refractoriness. Minimum separation times were got from the minimum AA interval.

In addition, we used activation mapping method to find the reentry, activated region, and spatial-temporal information. The activation mapping was a method to analyze the spatial-temporal pattern [21], [22]. Activation was characterized by unorganized and chaos activation with several simultaneously present activation waves. From observing the activation mapping, we can preliminarily understand the activation of tissue and the mechanism of the AF. Fig. 2 shows the baseline spatial-temporal patterns of subject P1 during 60–120 ms of the recordings. In the RA, there is an activated region near the SA node. In the LA, there are two to three activated regions near the center and one reentry happened on the top of the LA.

The number of wavelets in the LA is more than that in the RA. After that, we can calculate the gradient of the wavelets. The gradient is a vector field which points in the direction of the greatest rate of increase of the scalar field and whose magnitude is the greatest rate of change [23]. From the gradient of each electrogram, we can determine the myocardial activation direction and velocity, and find the activated region [the propagation velocity of the ionic is lower than the minimum conduction velocity (CV)]. Besides, the focus where the wavelet propagated from can also be observed [24].

B. Wavelet Detection

According to the multiple wavelet theory [25], an increased atrial refractory period results in a longer wavelength for the

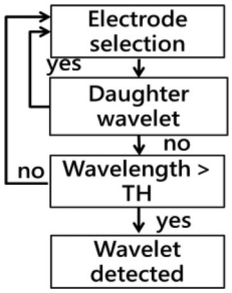

Fig. 3. Method of atrial wavelet detection. First, we choose the activated electrodes. Second, we check whether the electrode propagates to all neighborhoods or not. If the activity of the electrode successfully propagates to all neighborhoods and whose CV satisfies (1), it becomes the candidate of the wavelet. We then check if the wavelength activated from the candidate region is bigger than the threshold or not. Finally, the atrial wavelet was detected.

fibrillation wavelet. There will be fewer simultaneous wavelets in the atria. Because the size (wavelength) of the wavelet increases, this may increase the tendency toward termination of AF. Therefore, we used the wavelet number to estimate the therapeutic effect and the condition after the drug treatment.

Fig. 3 shows the method of the wavelet detection used in this study. First, we choose the electrodes having been activated. Second, whether activity of the electrode propagates to all neighborhoods or not was checked. If the activity of the electrode successfully propagates to the neighborhoods and whose CV satisfies the condition in

$$\text{CV} = \frac{3.5 \text{ mm}}{|A(i) - A(i)_n|} > \min \text{CV} \tag{1}$$

the electrode is regarded as the candidate region. In (1), $A(i)$ and $A(i)_n$ represent the ith activation time of the electrodes and the activation time of the neighbors of the electrode, respectively. If the wavelength activated from the candidate region is larger than the threshold, the wavelet is detected.

C. ARX Model

Our major interest is to develop a model to estimate the therapeutic effect and the condition after the treatment for AF. Since short-term predictability of RR interval in ventricular was demonstrated as the linear oscillators [26] and the medication globally suppress the activated reentry, the linear autoregressive model with exogenous inputs (ARX) is used to predict and estimate the condition after the pharmacologic treatment.

The ARX is a widely studied model in the control systems and can be defined by the following linear stochastic difference equation [27]:

$$\begin{aligned} y(k) &= \alpha_1 y(k-1) + \alpha_2 y(k-2) + \cdots + \alpha_p y(k-p) \\ &\quad + \beta_0 u(k) + \beta_1 u(k-1) + \beta_2 u(k-2) + \cdots \\ &\quad + \beta_p u(k-\text{p}) + \varepsilon(k) \end{aligned} \tag{2}$$

where $\{y(k)\}$, $\{u(k)\}$, $\{\varepsilon(k)\}$, and p denote the output, input, disturbance sequences, and the order of ARX model, respectively [27]. In our research, $u(1)$ to $u(L)$ is the AA interval sequence before the treatment, $y(1)$ to $y(L)$ is the AA interval sequence after the treatment, and L is the length of data, $u(j)$ and $y(j)$ are zero when $j \leqq 0$; the order of the ARX model is 2. Comparing the loss functions of the ARX models with orders from 2 to 20, the second-order ARX results the minimum loss function. When the input terms $\{u(k)\}$ are absent, (2) reduces to the classical autoregressive model (AR). The random disturbances are assumed to be independent and identically distributed with zero mean and variance σ^2. In many applications, $\{\varepsilon(k)\}$ are usually ignored. The coefficient matrices α_i and β_i are referred as the ARX parameters. The output measurement at time step k can be expressed as the weighted sum of its previous inputs and outputs. The determination of the weights can be performed based on the least mean square criteria.

In this paper, the ARX model was used to estimate the AA interval sequence after the treatment. In order to estimate the condition after pharmacological therapy, we use the AA interval sequence of one subject before and after the treatment to build the ARX model. Note that each electrode has an independent ARX model for simulation of drug processing; i.e., there are total 224 ARX models in this method.

After that, we use the AA interval sequence of one subject before the treatment as the input of the ARX model and obtain the estimated AA interval sequence of one subject after the treatment by the output of ARX model. By the estimated AA interval sequence, we can reconstruct the estimated activation time sequence. Finally, the estimated activation time sequence was utilized to calculate the estimated wavelet number.

For the training of ARX model, we can modify (2) into the following matrix form:

$$Y = PW + E \tag{3}$$

where

$$\begin{aligned} Y &= [y(L)y(L-1)\cdots y(1)] \\ P &= [\alpha_1 \alpha_2 \cdots \alpha_p \beta_0 \beta_1 \cdots \beta_p] \\ W &= \begin{bmatrix} y(L-1) & \cdots & y(0) \\ y(L-2) & \cdots & y(-1) \\ \vdots & \ddots & \vdots \\ y(L-p) & \cdots & y(1-p) \\ u(L) & \cdots & u(1) \\ u(L-1) & \cdots & u(0) \\ \vdots & \ddots & \vdots \\ u(L-p) & \cdots & u(1-p) \end{bmatrix}, \quad \text{and} \\ E &= [\varepsilon(L)\varepsilon(L-1)\cdots\varepsilon(1)]. \end{aligned}$$

P can be depend by the least-squares method

$$P = YW^{+} \tag{4}$$

where W^{+} is the pseudoinverse of W.

The flowchart of our proposed method is shown in Fig. 4. Our method consists of two parts: training part and testing part. In the training part, in order to estimate the wavelet number after the drug treatment, we used the AA interval sequence of one subject before and after the treatment to build the ARX model.

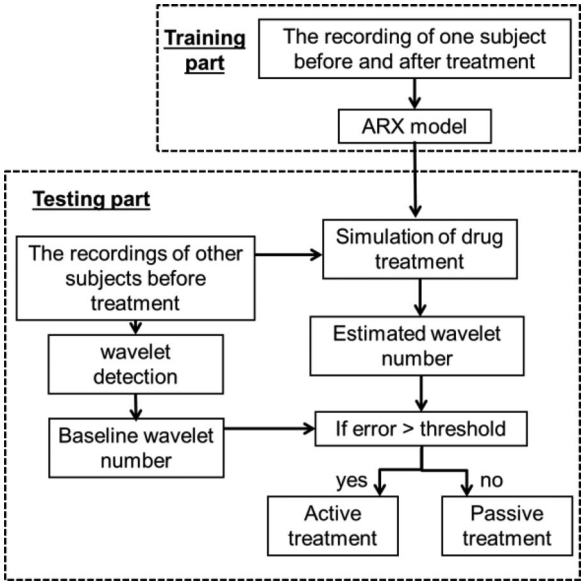

Fig. 4. Flowchart of the proposed method developed in this study. First, we use the AA interval sequence of one subject to build the ARX model. After constructing the model, it was used to subject-independently predict the wavelet number of each subject after drug, PPF or STL, treatment. If the difference between baseline and estimated wavelet number is larger than threshold, the treatment is regard as active treatment; otherwise, it is passive treatment.

Subjects P1 and P10 were used to build the ARX models for the PPF treatment and the STL treatment, respectively. In the testing part, after constructing the ARX models for PPF and STL treatments, the models were used to subject-independently predict the wavelet number of each subject after the drug treatment. If the difference between baseline and estimated wavelet number is larger than the threshold, the treatment is regard as active treatment; otherwise, it is passive treatment. The estimated results were compared with the recorded results for performance evaluation.

TABLE I
MEAN AA INTERVALS AND WAVELET NUMBERS OF THE SUBJECTS BEFORE AND AFTER THE PPF TREATMENT

Subject	Baseline (BL)		PPF		A/P
	mean AA interval	Wavelets	mean AA interval	Wavelets	
P1R	107.4	7.0	128.6	5.4	A
P1L	74.4	15.0	144.5	6.1	A
P2R	97.2	8.6	99.9	8.9	P
P2L	93.4	8.9	77.5	9.4	P
P3R	95.8	7.2	207.0	2.8	A
P3L	89.9	13.0	135.5	7.9	A
P4R	105.1	7.0	172.3	4.3	A
P4L	116.0	7.2	220.0	2.8	A
P5R	132.7	3.6	185.0	4.0	P
P5L	113.5	7.4	118.7	8.0	P

There were five pigs, marked as P1, P2, P3, P4, and P5, with sustained AF used in this study.

TABLE II
MEAN AA INTERVALS AND WAVELET NUMBERS OF THE SUBJECTS BEFORE AND AFTER THE STL TREATMENT

Subject	Baseline (BL)		STL		A/P
	mean AA interval	Wavelets	mean AA interval	Wavelets	
P6R	118.7	7.7	144.3	5.5	A
P6L	117.5	6.1	144.5	6.4	P
P7R	93.3	7.9	81.8	9.0	P
P7L	82.6	7.0	108.2	4.3	A
P8R	91.6	9.3	97.6	8.4	P
P8L	64.3	8.7	NA	NA	NA
P9R	117.3	6.6	117.6	6.7	P
P9L	100.4	8.6	100.5	7.0	A
P10R	88.9	8.9	169.6	3.4	A
P10L	82.3	10.9	106.2	6.4	A
P11R	96.6	7.4	218.4	3.3	A
P11L	78.9	12.4	131.9	5.9	A
P12R	114.1	7.1	126.7	5.9	A
P12L	106.0	7.4	109.5	6.7	A

There were seven pigs, marked as P6, P7, P8, P9, P10, P11, and P12, with sustained AF used in this study.

III. EXPERIMENTAL RESULTS

A. *Estimations of AA Intervals and Wavelet Numbers*

The mean AA interval and wavelet number of subjects before and after the treatment of PPF and STL administration are listed in Tables I and II, respectively. In Tables I and II, "R" and "L" indicate the data measured from the right and left atrium, respectively; "NA" indicates nonavailable data; "Baseline (BL)" shows the data measured before the treatment; and "PPF" and "STL" indicate the data measured after PPF and STL treatments, respectively. "A" and "P" designate the subjects regarded as active treatment and passive treatment, respectively. After the drug treatment, the subject was regarded as an active-treatment (A) subject if the increase of the mean AA interval and minimal acceptable atrial refractoriness as well as the decrease of the wavelet number were observed. Otherwise, the subject was regarded as a passive-treatment (P) subject [23].

PPF worked on six, P1 (P1R and P1L), P3 (P3R and P3L), and P4 (P4R and P4L), from ten subjects to become active subjects and STL worked on nine, P6R, P7L, P9L, P10 (P10R and P10L), P11 (P11R and P11L), and P12 (P12R and P12L), from 13 subjects to become active subjects. Obviously, we could not recognize whether the treatment is active or not by only the baseline wavelet number. For example, in the PPF treatment, P4L is active and its baseline wavelet number is 7.2. But P5L is passive and its baseline wavelet number (7.4) is very close to the baseline wavelet number of P4L. Similarly, in the STL treatment, P6R is active and its baseline wavelet number is 7.7. But P7R is passive and its baseline wavelet number (7.9) is also very close to the baseline wavelet number of P6R. Therefore, we used a mathematical model, ARX model, to simulate the process of drug treatment and estimate the result after PPF or STL treatment.

Moreover, we observed the occurrence of wavelet number in each electrode with a fixed period of time. After the treatment, the occurrence of wavelet number of the active treatment subjects is reduced in most of the electrodes. However, after the treatment, the occurrence of wavelet number of the passive treatment subjects is not decreased in most of the electrodes. Fig. 5(a) shows the comparison of wavelet number in each electrode of subject P3. The re-exciting of the wavelet in atrium is

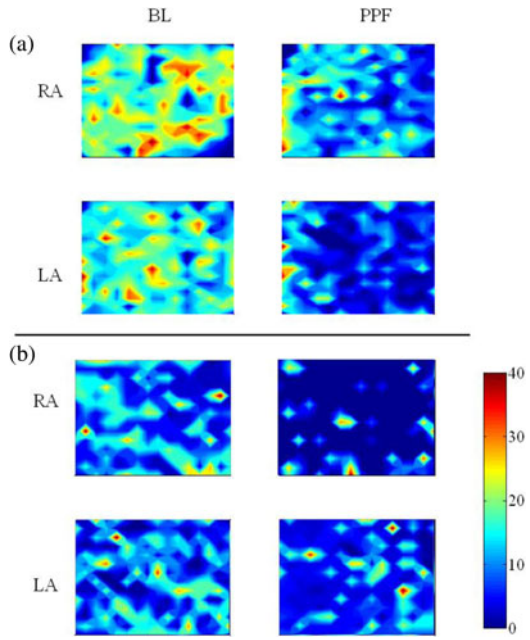

Fig. 5. Wavelet number activated from each site over 10 s. The color in the block represents the number of wavelet activated from the electrode in 10 s. The deep red represents that the wavelet activated from the electrode about 40 times. The deep blue represents that there was no wavelet activated from the electrode. (a) Data were from P3. After PPF, the wavelet number was reduced in most of the electrodes. (b) Data were from P5. After PPF, the wavelet number in LA was not reduced in most of the electrodes.

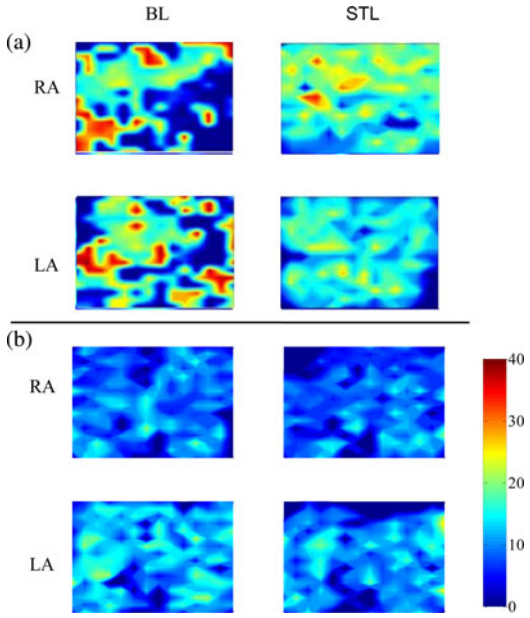

Fig. 6. Wavelet number activated from each electrode over 10 s. The deep red and deep blue represent the same mean as that used in Fig. 5. (a) Data were from P11. After STL, the wavelet number was reduced in most of the electrodes. (b) Data were from P9. After STL, the wavelet numbers in RA and LA were not reduced in most of the electrodes.

reduced after the treatment in P3. Fig. 5(b) shows the comparison of wavelet number in each electrode of subject P5. After the treatment, the re-exciting of the wavelets has a slight reduction in LA.

Similar to the PPF treatment, Fig. 6(a) shows the comparison of wavelet number in each electrode of subject P11. The re-exciting of the wavelet in atrium is reduced after the treatment in P11. Fig. 6(b) shows the comparison of wavelet number in each electrode of subject P9. After the treatment, the re-exciting of the wavelets in RA was not reduced.

In addition to the reduction of wavelet number shown in Tables I and II, comparing Fig. 5 with Fig. 6, it can be observed that the electrical activity after the PPF treatment is more regular than that after the STL treatment. This result is general in our experimental data.

B. Analysis and Prediction of Therapeutic Effect by PPF

From Table I, we could classify the active treatment and passive treatment subjects and that ARX model can be used to estimate the wavelet number of the subjects after the medication. We used the data of P1 whose relationship between baseline and PPF to build the model and other subjects as testing sets to estimate the condition of the PPF and validate the result. Table III(a) and (b) shows the results with respect to active and passive treatments, respectively. In Table III, "Treatment" indicates the recording wavelet numbers after the PPF treatment. "ARX" shows the estimated wavelet numbers after the PPF treatment by the ARX model. Estimated difference was defined as the difference between the baseline wavelet number and the estimated wavelet number after the PPF treatment. "Error" designates the error between the actual wavelet numbers after the PPF treatment and the estimated wavelet number after the PPF treatment. "MAE" represents the mean absolute error.

TABLE III
COMPARISON OF THE RECORDED AND ESTIMATED WAVELET NUMBER OF ALL SUBJECTS TREATED WITH PPF ADMINISTRATION

(a) Active subjects (ED < –2.5)

Subject	Baseline	Treatment	ARX	ED (ARX - Baseline)	Error (ARX - Treatment)
P1R†	7.0	5.4	3.2	-3.8	-2.2
P1L†	15.0	6.1	6.6	-8.4	0.5
P3R	7.2	2.8	4.6	-2.6	1.8
P3L	13.0	7.9	5.8	-7.2	-2.1
P4R	7.0	4.3	2.8	-4.2	-1.5
P4L	7.2	2.8	2.5	-4.7	-0.3
MAE					1.4
Mean	9.4	4.9	4.3	-5.2	

(b) Passive subjects (ED ≥ –2.5)

Subject	Baseline	Treatment	ARX	ED (ARX - Baseline)	Error (ARX - Treatment)
P2R	8.6	8.9	6.3	-2.3	-2.6
P2L	8.9	9.4	7.7	-1.2	-1.7
P5R	3.6	4.0	5.6	2.0	1.6
P5L	7.4	8.0	6.0	-1.4	-2.0
MAE					2.0
Mean	7.2	7.6	6.4	-0.7	

"†" represents the subject was used to build the ARX model.

According to Table III, some interesting and useful characteristics can be observed. The estimated wavelet number of the subject is similar to the original treatment result. The MAE is 1.4 in the active treatment and 2.0 in the passive treatment. The PPF treatment is active or not can be recognized by a threshold.

TABLE IV
COMPARISON OF THE RECORDED AND ESTIMATED WAVELET NUMBER OF ALL SUBJECTS TREATED STL ADMINISTRATION

(a) Active subjects (ED < -1.7)

Subject	Baseline	Treatment	ARX	ED (ARX - Baseline)	Error (ARX - Treatment)
P6R	7.7	5.5	4.1	-3.6	-1.4
P7L	7.0	4.3	5.2	-1.8	0.9
P9L	8.6	7.0	6.0	-2.6	-1.0
P10R†	8.9	3.4	5.2	-3.7	1.6
P10L†	10.9	6.4	5.1	-5.8	-1.3
P11R	7.4	3.3	2.8	-4.6	-0.5
P11L	12.4	5.9	6.7	-5.7	0.8
P12R	7.1	5.9	4.0	-3.1	-1.9
P12L*	7.4	6.8	6.7	-0.7	-0.1
MAE					1.0
Mean	8.6	5.4	5.1	-3.5	

(b) Passive subjects (ED ≥ -1.7)

Subject	Baseline	Treatment	ARX	ED (ARX - Baseline)	Error (ARX - Treatment)
P6L	6.1	6.4	5.4	-0.7	-1.0
P7R	7.9	9.0	6.2	-1.7	-2.8
P8R	9.3	8.4	8.3	-1.0	-0.1
P9R	6.6	6.7	7.7	1.1	1.0
MAE					1.2
Mean	7.5	7.6	6.9	-0.6	

"*" indicates the error predicting subject.

By setting the threshold as -2.5, the predicting accuracy correct rate is 100%. In addition, the prediction error of the estimated result is in the range of -2.6 to 1.8. It demonstrates that the ARX model can successfully estimate the wavelet number of the subject after the PPF treatment and forecast whether the PPF treatment is active or not.

C. Analysis and Prediction of the Therapeutic Effect by STL

Similar to the PPF treatment, the data of P10 corresponding to baseline and STL treatment were used to build the ARX model to estimate the wavelet number of other subjects after the STL medication. Table IV(a) and (b) shows the results with respect to active and passive treatments, respectively. The terms used in Table IV were similar to those in Table III.

According to Table IV, we could observe some characteristics like the results from the PPF treatment. The estimated wavelet number of the subject is also similar to the original treatment result. The MAEs are 1.0 and 1.2 in active and passive treatments, respectively. The STL treatment is active or not could also be recognized by a threshold. If the threshold is set as -1.7, the predicting accuracy rate is 92% (12/13). Although the predicting accuracy rate is not 100%, our proposed method still can be adopted since only P12L is misclassified. In addition, the prediction error of the estimated result is in the range of -2.8 to 1.6. The width of the range (4.4) is the same as the PPF result. The results demonstrate that the ARX model can also successfully estimate the wavelet number of the subject after the STL treatment and forecast whether the STL treatment is active or not.

IV. DISCUSSION AND CONCLUSION

In this study, we developed a predictive method to simulate the medication effect and forecast the condition after the treatment based on the ARX model. This paper is the first study to predict whether the drug treatment for AF is active or not. The main contributions of our study are to estimate the wavelet number after treatment and have high accuracy of prediction by using the ARX model. The ARX model has proved a good model for the simulating process of pharmacologic treatment.

In order to estimate the condition after pharmacological therapy, we use the AA interval sequence of one subject before and after the treatment to build the ARX model. After that, we use the AA interval sequence of one subject before the treatment as the input of the ARX model and obtain the estimated AA interval sequence of one subject after the treatment by the output of the ARX model. By the estimated AA interval sequence, we can reconstruct the estimated activation time sequence. Finally, the estimated activation time sequence was utilized to calculate the estimated wavelet number.

We used the original wavelet number to validate the result. In the PPF treatment, the MAEs of active, passive, and all subjects ($n = 10$) are 1.4, 2.0, and 1.6, respectively. In the STL treatment, the MAEs of active, passive, and all subjects ($n = 13$) are 1.0, 1.2, and 1.1, respectively. The MAEs corresponding to the PPF and STL are less than 2. It is shown that the predicting wavelet number is very close to the recording wavelet number. In addition, the estimated performance of active treatment is better than that of passive treatment and the estimated wavelet numbers are smaller than the baseline wavelet numbers, except P5R and P9R. This may be because the original AA intervals of passive subjects are less-regulated.

The ARX model not only gives the method to estimate wavelet number after the pharmacologic treatment, but can also predict whether the treatment is active or not. According to Tables III and IV, we set the two thresholds, -2.5 and -1.7, corresponding to whether the PPF and STL treatments are active or not, respectively. In addition to P12L, others are correct prediction; this may be because there is not much difference between baseline and recording wavelet number in active treatment's point of view. Moreover, the difference between baseline and the estimated wavelet number in the active treatment is bigger than that in the passive treatment. The predicting accuracy rates corresponding to the PPF and STL treatments are 100% and 92%, respectively. The results mean that the ARX model can effectively predict and estimate the situations after PPF and STL treatments so that the subjects can also be correctly categorized as active subjects, no matter whether the treatment is active or not.

In order to know that how representative are the multielectrode recordings, we redo our experiment with only used electrodes' number of the electrode array to two and four widely separate electrodes. In other words, 56 ($7 * 8$)- and 12 ($3 * 4$)-site electrodes' data were used, respectively. The training data for PPF and STL model are the same as our original experiment setting (P1 for PPF and P10 for STL). The results of analysis and prediction of the therapeutic effect by PPF and STL are shown in Fig. 7. The results show that the predictive accuracy does

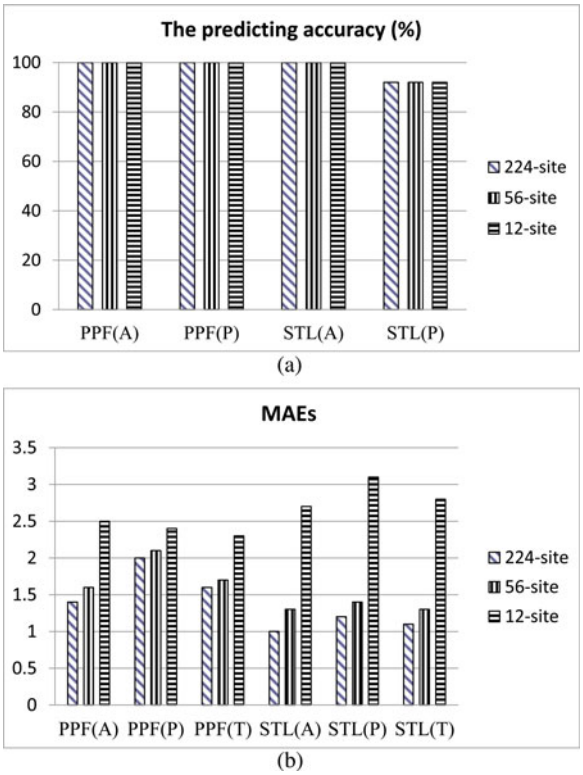

Fig. 7. (a) Predicting accuracy rate and (b) MAEs with using different electrode number. PPF(A), PPF(P), and PPF(T) represent the active subject, passive subject, and total subject with the PPF treatment, respectively. STL(A), STL(P), and STL(T) represent the active subject, passive subject, and total subject with the STL treatment, respectively.

not decrease if we reduce the number of electrodes to 56 or 12 electrodes. However, the MAEs would increase if the number of electrodes were reduced. Moreover, the wavelet of passive subjects should be increase after the drug treatment. Under this situation, it does not make any sense even if predicting accuracy rate is 100%.

Frequency mapping rapidly and accurately identifies the region of dominant activation frequency. The frequency is faster and more variable in AF subjects. The scar, fibrosis, and the type of AF can really affect the dominant frequency, pattern, and location. In spite of the histological characteristics in the fibrillating atria of pigs induced by rapid atrial pacing were similar but uncomplicated to those seen in humans. Increased interstitial was fibrosis found in the fibrillating atrial of pigs, but no large regions of myocardial fibrosis were identified [20]. The pigs were used in this study when the sustained AF was just induced for 3 days; therefore, the significant scar/fibrosis injury did not formatted. Additionally, when the epicardial mapping performed, the plaque electrode array was set to a stable position on the atrial surface of pigs. That is why a stable location of dominant frequency could be measured in most of the epicardial mapping in our pigs; however, about half the patients with AF showed that the location of dominant frequency was unstable, changing during the recording period [28].

In the pharmacologic treatment, PPF make atrial rhythm slower and more regular [5] and STL significantly increased the effective refractory period [9]. In our dataset, after the active PPF treatment, we can know that the wavelet and electrical activity become more regular by activation mapping. PPF makes the disordered wavelet propagation into a more regular way of propagation. Moreover, the activation mappings of subjects between before and after the STL treatment do not have much difference. Our results of activation mapping and the characteristic of PPF and STL were consistent. The activation mapping not only gives us a rudimentarily understanding of the AF mechanism, but also help the doctor to choose the activated region when use the nonpharmacologic treatment, i.e., catheter ablation [29]–[31].

Epicardial mapping of swine electrograms was used in this study. Although the principles demonstrated in this study are also applicable to human endocardial recordings, the relative importance and magnitude on AF may differ. AF is caused by rapidly discharging, spontaneously active, and atrial ectopic foci by a multiple reentry circuits. In clinical, several heart diseases, such as CHF, CABG, and mitral valve disease, may change the architecture of atrial tissue, causing a substantial increase in fibrosis of atrial tissues, which interferes with electrical conduction and causes AF. In our pig model, increasing extracellular matrix (ECM) was found in the porcine atria with fibrillation induced by rapid atrial pacing for 4–6 weeks. We have proposed that increased expression of ECM proteins in fibrillating atria supports the hypothesis that ECM metabolism contributes to the development of AF [20], [32]. We have further investigated that the remodeling of atrial ECM in AF involves changes in the expression of matrix metalloproteinases (MMPs) and tissue inhibitors of MMPs (TIMPs) [33]. Although fibrotic islets in the atria have not been identified, tissue fibrosis in the fibrillating atria as an effect would be included in our established model.

We acknowledge the limitation that long-term operation of epicardial mapping is difficult to be performed in animal models; however, the sustained AF of pigs (AF $\geq$ 72 h) was confirmed by ECG and even by Doppler echocardiographic check before the pigs received thoracotomy for epicardial mapping. Therefore, we proposed that the atrial electrophysiological features of AF were sustained and stable.

In the future, in order to get the statistical results to confirm the robustness of our approach, more experiments on data of the swine or other models were required. Because the structure of swine heart is similar with the human, it is expected that our approach can be applied to humans. There are many aspects that should to be addressed until this approach might be applied in patients. For example, several antiarrhythmic drugs being of clinical relevance that should been tested and human data need to be tested for the validity of our proposed method. It is expected that the developed model can be further extended to assist the clinical staffs to choose the effective treatment for the AF patients in the future.

ACKNOWLEDGMENT

The authors would like to thank J.-L. Lin and L.-P. Lai at the Division of Cardiology, Department of Internal Medicine, National Taiwan University Hospital, Taipei, Taiwan, for providing the data of swine models and their valuable comments on the study.

REFERENCES

[1] C. D. Furberg, B. M. Psaty, T. A. Manolio, J. M. Gardin, V. E. Smith, and P. M. Rautahariju, "Prevalence of AF in elderly subjects (the cardiovascular health study)," *Amer. J. Cardiol.*, vol. 74, pp. 236–241, 1994.

[2] W. B. Kannel, P. A. Wolfs, E. J. Benjamin, and D. Levy, "Prevalence, incidence, prognosis, and predisposing conditions for AF: Population-based estimates," *Amer. J. Cardiol.*, vol. 82, pp. 2N–9N, 1998.

[3] S. Stewart, C. L. Hart, D. L. Hole, and J. J. McMurray, "Population prevalence, incidence, and predictors of AF in the renfrew/paisley study," *Heart*, vol. 86, pp. 516–521, 2001.

[4] R. G. Hart and J. L. Halperin, "AF and stroke: Concepts and controversies," *Stroke*, vol. 32, pp. 803–808, 2001.

[5] V. Fuster, L. E. Rydén, D. S. Cannom, H. J. Crijns, A. B. Curtis, K. A. Ellenbogen, J. L. Halperin, J.-Y. Le Heuzey, G. N. Kay, J. E. Lowe, S. B. Olsson, E. N. Prystowsky, J. L. Tamargo, S. Wann, S. C. Smith, A. K. Jacobs, C. D. Adams, J. L. Anderson, E. M. Antman, S. A. Hunt, R. Nishimura, J. P. Ornato, R. L. Page, B. Riegel, S. G. Priori, J.-J. Blanc, A. Budaj, A. J. Camm, V. Dean, J. W. Deckers, C. Despres, K. Dickstein, J. Lekakis, K. McGregor, M. Metra, J. Morais, A. Osterspey, and J. L. Zamorano, "ACC/AHA/ESC 2006 guidelines for the management of patients with AF," *J. Am. Coll. Cardiol.*, vol. 4, no. 48, pp. 149–246, 2006.

[6] E. N. Prystowsky, "Management of AF: Therapeutic options and clinical decisions," *Amer. J. Cardiol.*, vol. 85, no. 10A, pp. 3D–11D, 2000.

[7] L. D. Dennis, M. L. Greenberg, P. T. Holzberger, D. J. Malenka, and J. D. Birkmeyer, "Managing chronic AF: A Markov decision analysis comparing warfarin, quinidine, and low-dose amiodarone," *Ann. Intern. Med.*, vol. 120, pp. 449–457, 1994.

[8] J. Wang, G. W. Bourne, and Z. Wang, "Comparative mechanisms of antiarrhythmic drug action in experimental atrial fibrillation: Importance of use-dependent effects on refractoriness," *Circulation*, vol. 88, pp. 1030–1044, 1993.

[9] H. F. Tse and C. K. Lau, "Electrophysiologic actions of DL-sotalol in patients with persistent AF," *J. Amer. Coll. Cardiol.*, vol. 40, pp. 2150–2155, 2002.

[10] V. Fuster, L. E. Rydén, R. W. Asinger, D. S. Cannom, H. J. Crijns, R. L. Frye, J. L. Halperin, G. N. Kay, W. W. Klein, S. Lévy, R. L. McNamara, E. N. Prystowsky, L. S. Wann, D. G. Wyse, R. J. Gibbons, E. M. Antman, J. S. Alpert, D. P. Faxon, G. Gregoratos, L. F. Hiratzka, A. K. Jacobs, R. O. Russell, S. C. Jr, Smith, W. W. Klein, A. Alonso-Garcia, C. Blomström-Lundqvist, G. de Backer, M. Flather, J. Hradec, A. Oto, A. Parkhomenko, S. Silber, and A. Torbicki, "ACC/AHA/ESC guidelines for the management of patients with atrial fibrillation: Executive summary a report of the American college of cardiology/American heart association task force on practice guidelines and the European society of cardiology committee for practice guidelines and policy conferences (committee to develop guidelines for the management of patients with atrial fibrillation) developed in collaboration with the North American Society of pacing and electrophysiology," *Circulation*, vol. 104, pp. 2118–2150, 2001.

[11] I. Faes, G. Nollo, M. Kirchner, E. Olivetti, F. Gaita, R. Riccardi, and R. Antolini, "Principal component analysis and cluster analysis for measuring the local organisation of human AF," *Med. Biol. Eng. Comput.*, vol. 39, pp. 656–663, 2001.

[12] R. Sun and Y. Wang, "Predicting termination of atrial fibrillation based on the structure and quantification of the recurrence plot," *Med. Eng. Phys.*, vol. 30, pp. 1105–1111, 2008.

[13] S. M. Narayan and V. Bhargava, "Temporal and spatial phase analyses of the electrocardiogram stratify intra-atrial and intra-ventricular organization," *IEEE Trans. Biomed. Eng.*, vol. 10, no. 51, pp. 1749–1764, Oct. 2004.

[14] G. Sugihara and R. M. May, "Nonlinear forecasting as a way of distinguishing chaos from measurement error in time series," *Nature*, vol. 344, pp. 734–741, 1990.

[15] B. P. Hoekstra, C. G. Diks, M. A. Allessie, and J. DeGoede, "Nonlinear analysis of epicardial atrial electrograms of electrically induced atrial fibrillation in man," *J. Cardiovasc. Electrophysiol.*, vol. 6, pp. 419–440, 1995.

[16] M. Costa, A. L. Goldberger, and C. K. Peng, "Multiscale entropy analysis of complex physiologic time series," *Phys. Rev. Lett.*, vol. 89, pp. 068102-1–068102-4, 2002.

[17] M. Mase, L. Faes, R. Antolini, M. Scaglione, and F. Ravelli, "Quantification of synchronization during atrial fibrillation by shannon entropy: Validation in patients and computer model of atrial arrhythmias," *Physiol. Meas.*, vol. 26, pp. 911–923, 2005.

[18] F. Nilsson, M. Stridh, A. Bollmann, and L. Sörnmoa, "Predicting spontaneous termination of atrial fibrillation using the surface ECG," *Med. Eng. Phys.*, vol. 28, pp. 802–808, 2006.

[19] J. L. Lin, L. P. Lai, C. S. Lin, C. C. Du, T. J. Wu, S. P. Chen, W. C. Lee, P. C. Yang, Y. Z. Tseng, W. P. Lien, and S. K. S. Huang, "Electrophysiological mapping and histological examinations of the swine atrium with sustained (>24 h) AF: A suitable animal model for studying human AF," *Cardiology*, vol. 99, pp. 78–84, 2003.

[20] C. S. Lin, L. P. Lai, J. L. Lin, Y. L. Sun, C. W. Hsu, C. L. Chen, S. J. T. Mao, and S. K. S. Huang, "Increased expression of extracellular matrix proteins in rapid atrial pacing-induced atrial fibrillation," *Heart Rhythm*, vol. 4, pp. 938–949, 2007.

[21] K. T. Konings, C. J. Kirchhof, J. R. Smeets, H. J. Wellens, O. C. Penn, and M. A. Allessie, "High-density mapping of electrically induced AF in humans," *Circulation*, vol. 89, pp. 1665–1680, 1994.

[22] R. Mandapati, A. Skanes, J. Chen, O. Berenfeld, and J. Jalife, "Stable microreentrant sources as a mechanism of AF in the isolated sheep heart," *Circulation*, vol. 101, no. 2, pp. 194–199, 2000.

[23] X.-F. Pang and M.-Y. Pang, "A tracing algorithm for intersection of parametric surface and implicit surface," in *Proc. Int. Conf. Wireless Netw. Inf. Syst.*, Dec. 2009, pp. 245–248.

[24] J. J. Rieta, F. Castells, C. Sánchez, V. Zarzoso, and J. Mille, "Atrial activity extraction for atrial fibrillation analysis using blind source separation," *IEEE Trans. Biomed. Eng.*, vol. 51, no. 7, pp. 1176–1186, Jul. 2004.

[25] G. K. Moe, "On the multiple wavelet hypothesis of atrial fibrillation," *Archives Int. Pharm. Therapie*, vol. 140, pp. 183–188, 1962.

[26] M. S. Kenneth, W. Jeff, L. Neal, and B. L. Bruce, "Ventricular response in atrial fibrillation: Random or deterministic?" *Amer. J. Physiol.*, vol. 277, pp. H452–H458, 1999.

[27] L. Ljung, *System Identification*, 2nd ed. Englewood Cliffs, NJ: Prentice-Hall, 1999.

[28] R. B. Schuessler, M. W. Kay, S. J. Melby, B. H. Branham, J. P. Boineau, and R. J. DamianoJr., "Spatial and temporal stability of the dominant frequency of activation in human atrial fibrillation," *J. Electrocardiol.*, vol. 39, pp. S7–S12, 2006.

[29] K. Nademanee, J. McKenzie, E. Kosar, M. Schwab, B. Sunsaneewitayakul, T. Vasavakul, C. Khunnawat, and T. Ngarmukos, "A new approach for catheter ablation of atrial fibrillation: Mapping of the electrophysiologic substrate," *J. Amer. Coll. Cardiol.*, vol. 43, pp. 2044–2053, 2004.

[30] H. Oral, A. Chugh, E. Good, S. Sankaran, S. S. Reich, P. Igic, D. Elmouchi, D. Tschopp, T. Crawford, S. Dey, A. Wimmer, K. Lemola, K. Jongnarangsin, F. Bogun, F. Jr. Pelosi, and F. Morady, "A tailored approach to catheter ablation of paroxysmal atrial fibrillation," *Circulation*, vol. 113, pp. 1824–1831, 2006.

[31] H. Oral, A. Chugh, E. Good, A. Wimmer, S. Dey, N. Gadeela, S. Sankaran, T. Crawford, J. F. Sarrazin, M. Kuhne, N. Chalfoun, D. Wells, M. Frederick, J. Fortino, S. Benloucif-Moore, K. Jongnarangsin, F. Jr. Pelosi, F. Bogun and F. Morady, "Radiofrequency catheter ablation of chronic atrial fibrillation guided by complex electrograms," *Circulation*, vol. 115, pp. 2606–2612, 2007.

[32] C. H. Pan, J. L. Lin, L. P. Lai, C. L. Chen, S. K. S. Huang, and C. S. Lin, "Downregulation of angiotensin converting enzyme II is associated with pacing-induced sustained atrial fibrillation," *FEBS Lett.*, vol. 581, pp. 526–534, 2007.

[33] C. L. Chen, S. K. Huang, J. L. Lin, L. P. Lai, S. C. Lai, C. W. Liu, W. C. Chen, C. H. Wen, and C. S. Lin, "Upregulation of matrix metalloproteinase-9 and tissue inhibitors of metalloproteinases in rapid atrial pacing-induced atrial fibrillation," *J. Mol. Cell. Cardiol.*, vol. 45, pp. 742–753, 2008.

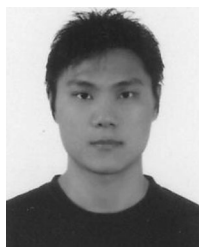

Chih-En Kuo was born in Tainan, Taiwan, in 1983. He received the B.S. degree in mathematics from the National Cheng Kung University, Tainan, Taiwan, and the M.S. degree in information management from the National Taiwan University of Science and Technology, Taipei, Taiwan, in 2005 and 2009, respectively. He is currently working toward the Ph.D. degree with the Department of Computer Science and Information Engineering, National Cheng Kung University.

His research interests include biomedical signal processing, algorithm analysis, human sleep EEG analysis, and automatic sleep staging.

Sheng-Fu Liang (M'09) was born in Tainan, Taiwan, in 1971. He received the B.S. and M.S. degrees in control engineering and the Ph.D. degree in electrical and control engineering from the National Chiao Tung University (NCTU), Hsinchu, Taiwan, in 1994, 1996, and 2000, respectively.

From 2001 to 2005, he was a Research Assistant Professor in electrical and control engineering at NCTU. He joined the Department of Biological Science and Technology, NCTU, in 2005 and joined the Department of Computer Science and Information Engineering (CSIE) and the Institude of Medical Informatics (IMI), National Cheng Kung University (NCKU), Tainan, Taiwan, in 2006. He is currently an Associate Professor in CSIE and IMI, NCKU. He is also a collaborative researcher of Biomimatic Systmes Research Center, NCTU. His current research interests include neural engineering, biomedical engineering, biomedical signal/image processing, machine learning, and medical informatics.

Shao-Sheng Lu was born in Taichung, Taiwan, in 1984. He received the B.S. and M.S. degrees from National Cheng Kung University, Tainan, Taiwan, in 2005 and 2008, respectively, both in computer science and information engineering.

He is currently a engineer with Wistron Corporation, Taipei, Taiwan. His research interests include biomedical engineering, biomedical signal/image processing, and analysis.

Tang-Ching Kuan received the B.S. and M.S. degrees in biomedical engineering from the I-SHOU University, Kaohsiung, Taiwan, in 2004 and 2006, respectively. He is currently working toward the Doctoral degree in the Department of Biological Science and Technology, National Chiao-Tung University, Hsinchu, Taiwan, focusing on the association with ACE2, MMPs, and heart remodeling.

Chich-Sheng Lin received the Ph.D. degree from the Department of Animal Science, National Chung Hsing University, Taichung, Taiwan, in 1998.

He is currently a Professor with the Department of Biological Science and Technology, National Chiao-Tung University, Hsinchu, Taiwan. He has authored/coauthored more than 85 scientific publications and filed 12 patents. His research spans several fields, including biological medicine to investigate the molecular pathogenesis of fibrotic diseases in heart and lung, and biosensing technology for the detection of pathogens and biomarkers.